NIH Public Access
Author Manuscript
Cancer Res. Author manuscript; available in PMC 2015 June 15.

Published in final edited form as:
Cancer Res. 2014 June 15; 74(12): 3271–3281. doi:10.1158/0008-5472.CAN-13-2015.

Novel polymeric nanoparticles for intracellular delivery of peptide cargos: antitumor efficacy of the Bcl-2 conversion peptide NuBCP-9

Manoj Kumar[1], **Dikshi Gupta**, **Gurpal Singh**[1], **Sapna Sharma**[1], **Madhusudan Bhatt**[2], **C.K. Prashant**[2], **A.K. Dinda**[2], **Surender Kharbanda**[3], **Donald Kufe**[3,*], and **Harpal Singh**[1,*]

[1]Center for Biomedical Engineering, Indian Institute of Technology, Hauz Khas, New Delhi-110016, India

[2]Department of Pathology, All India Institute of Medical Sciences, Ansari Nagar New Delhi-110029, India

[3]Department of Medical Oncology, Dana-Farber Cancer Institute, Harvard Medical School, Boston, MA 02215

Abstract

The preclinical development of peptidyl drugs for cancer treatment is hampered by their poor pharmacological properties and cell penetrative capabilities in vivo. In this study, we report a nanoparticle-based formulation that overcomes these limitations, illustrating their utility in studies of the anti-cancer peptide NuBCP-9 which converts BCL-2 from a cell protector to a cell killer. NuBCP-9 was encapsulated in polymeric nanoparticles (NPs) comprised of a polyethylene glycol (PEG)-modified polylactic acid diblock copolymer (NuBCP-9/PLA-PEG), or PEG-polypropylene glycol-PEG-modified PLA - tetrablock copolymer (NuBCP-9/PLA-PEG-PPG-PEG). We found that peptide encapsulation was enhanced by increasing the PEG chain length in the block copolymers. NuBCP-9 release from the NPs was controlled by both PEG chain length and the PLA molecular weight, permitting time-release over sustained periods. Treatment of human cancer cells with these NPs in vitro triggered apoptosis by NuBCP-9-mediated mechanism, with a potency similar to NuBCP-9 linked to a cell-penetrating poly-Arg peptide. Strikingly, in vivo administration of NuBCP-9/NPs triggered complete regressions in the Ehrlich syngeneic mouse model of solid tumor. Our results illustrate an effective method for sustained delivery of anticancer peptides, highlighting the superior qualities of the novel PLA-PEG-PPG-PEG tetrablock copolymer formulation as a tool to target intracellular proteins.

Keywords

BCL-2; NuBCP-9; apoptosis; nanoparticles; therapeutic peptides

[*]Corresponding authors..

Conflict of Interest: The authors disclose no conflict of interest.

NIH-PA Author Manuscript
NIH-PA Author Manuscript
NIH-PA Author Manuscript

NIH-PA Author Manuscript

NIH-PA Author Manuscript

NIH-PA Author Manuscript

Introduction

BCL-2 family proteins are important regulators of the mitochondrial outer membrane potential (MOMP) and thereby the induction of apoptosis (1, 2). The BCL-2 family is divided into proapoptotic and antiapoptotic members that share BCL-2 homology (BH) domains. The proapoptotic BCL-2 family members BAX and BAK contain multiple BH domains and control the MOMP. Other proapoptotic members that possess only the BH3 domain (BAD, BIM, BID, PUMA, and NOXA) either directly activate BAX/BAK, or inhibit the antiapoptotic activity of BCL-2 and BCL-xL to promote BAX/BAK activation. The antiapoptotic activities of the BCL-2 and BCL-xL proteins have been targeted with peptides derived from the BH3 domain and with small molecule inhibitors, such as ABT-737 and navitoclax, that mimic the BH3 alpha-helix (3-5). BCL-2 has also been targeted with a Nur77-derived peptide of 9 amino acids (NuBCP-9) (6). Nur77 is an orphan nuclear receptor that interacts with the BCL-2 N-terminal loop region and induces a BCL-2 conformational change (7). Binding of Nur77 exposes the BCL-2 BH3 domain and converts BCL-2 from an antiapoptotic protein to an inducer of apoptosis (7). Based on these findings, the D-amino acid NuBCP-9 peptide corresponding to the Nur77 region that interacts with BCL-2 was conjugated to the cell-penetrating DArg octamer (r8). Significantly, NuBCP-9-r8 was shown to induce apoptosis of cancer, but not normal, cells by a BCL-2-dependent mechanism (6). As predicted from Nur77 studies, NuBCP-9 binding was associated with a BCL-2 conformational change and thereby neutralization of BCL-2-mediated inhibition of BAX (6). NuBCP-9 binding to BCL-2 also exposes the BCL-2 BH3 domain and inhibits the survival function of BCL-xL (6). These findings and the demonstration that NuBCP-9-r8 induces apoptosis of cancer cells in vitro and in animal models supported the development of NuBCP-9-r8 as a selective anti-cancer agent.

Intracellular cancer targets that are devoid of an ATP binding pocket are often undruggable with small chemical inhibitors. Cell-penetrating therapeutic peptides have thus emerged as promising agents because of their potential for targeting intracellular proteins in cancer cells with high specificity and limited off-target toxicity (8, 9). However, delivery of anti-cancer peptides presents a challenge as a result of the potential degradation and immunogenicity of these agents. In addition, small therapeutic peptides generally have short circulating half-lives and require frequent administration for sustained inhibition of their target proteins (10). Therapeutic peptides also frequently require a protein transduction domain (PTD) for cell membrane penetration and intracellular localization (11-13). Cell-penetrating peptides (CPPs) that have been widely used for cargo delivery include, among others, the TAT peptide, penetratin and oligoarginines (11). The selection of a certain CPP is of importance in that the CPP can in a cargo-dependent manner contribute to decreased serum stability, inefficient transit from the endosome to the cytosol and unanticipated toxicities (14). Indeed, for NuBCP-9, the cell-penetrating r8 used for intracellular delivery acts in synergy with the N-terminal phenylalanine of NuBCP-9 to cause membrane blebbing and cell necrosis that are independent of BCL-2 expression (15). These findings have supported the study of alternative CPPs for NuBCP-9 or other formulations that preclude the use of a CPP for intracellular delivery.

NIH-PA Author Manuscript

NIH-PA Author Manuscript

NIH-PA Author Manuscript

Nanoparticle (NP) delivery systems for anti-cancer agents, particularly small molecules such as doxorubicin and paclitaxel, have been developed to improve pharmacokinetic parameters and therapeutic index (16). In this context, tumor microenvironments that are subject to hypoxia and acidosis can limit the effectiveness of small molecule anti-cancer agents (16). By extension and through what is referred to as the enhanced permeation retention (EPR) effect, NP delivery of anti-cancer agents can overcome limitations imposed by the tumor microenvironment and sustain drug exposure (16, 17). NPs can also be decorated with ligands to selectively target the surface of tumor cells (18). Polymeric NPs represent one class that has been widely studied and shown to be non-toxic, biocompatible and biodegradable (19, 20). Specifically, PLA-PEG block copolymer NPs have been used as carriers for anti-cancer drugs in sustained/controlled release and targeted delivery systems to enhance efficacy and circumvent drug resistance (19, 20). For example, Genexol-PM is a paclitaxel-loaded PLA-PEG polymeric NP that is approved for use in Korea and is undergoing Phase II evaluation in the United States for metastatic cancers (19, 21). BIND Biosciences also has under development docetaxel-encapsulated PLA-PEG NPs for the treatment of solid tumors (19). Curiously, polymeric NPs have not been fully evaluated for the delivery of anti-cancer peptide drugs.

The present studies have focused on the encapsulation of NuBCP-9 into PLA-PEG NPs or a novel PLA-PEG-PPG-PEG tetrablock NP system to assess delivery of this anti-cancer peptide to malignant cells in vitro and in vivo. The results obtained provide the experimental basis for the further development of NuBCP-9/NPs and for the potential delivery of other anti-cancer peptide drugs.

Materials and Methods

Synthesis and characterization of PLA-PEG copolymers

PLA-PEG diblock copolymers were synthesized using 72 kDa PLA (NatureWorks, Blair, NE) or ~12 kDa PLA (Purac Chemicals, Netherlands). PEG was used at 1, 2 or 4 kDa (CDH, Mumbai, India) for coupling to PLA. PEG-PPG-PEG (12.5 kDa; Poloxamer-F127, Sigma-Aldrich, St. Louis, MO) was also used for the synthesis of PLA block copolymers. In a standard experiment, 0.014 mmol PLA and PEG or PEG-PPG-PEG were dissolved in 100 ml dichloromethane (CH_2Cl_2) and stirred at 0–2°C. To these solutions, 5 ml of 1% N,N-dicyclohexylcarbodimide (DCC) was added slowly, followed by the addition of 2 ml of 0.1% 4-dimethylaminopyridine (DMAP) and stirring for 16 h. The resulting PLA-PEG and PLA-PEG-PPG-PEG block copolymers were precipitated with a 1:1 mixture of diethyl ether and methanol to remove unreacted PEG and PEG-PPG-PEG. Gel permeation chromatography (GPC) analysis was performed at room temperature using a Viscoteck GPC system with THF as the mobile phase. The synthesized PLA block copolymers were dried under vacuum and stored at –20°C until use. ^{1}HNMR of PLA-PEG or PLA-PEG-PPG-PEG was performed in $CDCl_3$ at 300 Hz (Bruker, Germany).

Preparation of Rhodamine B and NuBCP-9 loaded NPs

Loading of the PLAPEG and PLA-PEG-PPG-PEG NPs was performed using a double emulsion solvent evaporation method. PLA-PEG or PLA-PEG-PPG-PEG copolymers (100

NIH-PA Author Manuscript

NIH-PA Author Manuscript

NIH-PA Author Manuscript

mg) were dissolved in 5 ml acetonitrile. Rhodamine B (1 mg) or L-amino acid NuBCP-9 (10 mg; BioConcept, Gurgaon, India) was added to the solution with brief sonication. The resulting primary emulsion was then added dropwise into a 20 ml aqueous phase comprised of Poloxamer-F127 (PEG-PPG-PEG) in distilled water and stirred at room temperature for 6-8 h to facilitate solvent evaporation and NP stabilization. NPs were loaded with NuBCP-9 (FSRSLHSLL) peptide (7) and filtered through an Amikon 10 kDa ultra-filter (Millipore, Billerica, MA). The NPs were lyophilized and stored at –20°C until use. The filtrate was collected and analyzed for free NuBCP-9 peptide using a micro BCA kit (Pierce Chemicals, Rockford, IL). Encapsulation efficiency of NuBCP-9 peptide was determined using the following formula:

$$EE\,(\%) = \frac{(\text{Peptide})\,\text{Total} - (\text{Peptide})\,\text{Filtrate}}{(\text{Peptide})\,\text{Total}} \times 100$$

Morphology and particle size of the NPs was determined using a Zeiss EVO 50 Series Scanning Electron Microscope (SEM). Zeta-potential of the NPs was assessed by nanoparticle tracking analysis (NTA; NanoSight NS500, Cambridge, UK).

Assessment of NuBCP-9 release from NPs

The in vitro release kinetics of NuBCP-9 from NPs were determined by the ultrafiltration method. Briefly, samples of freeze dried NPs (10 mg) were suspended in PBS and incubated at 37°C with gentle shaking at 150-160 rpm. At pre-determined time points over 60 d, the samples were removed from the incubator and ultra-filtered through 10 kDa Amikon filters (Millipore). The filtrates were collected for analysis and fresh buffer was added to the respective tubes. Peptide concentration in the filtrates was determined by micro BCA assay.

Cell culture

Human MCF-7 breast cancer and HepG2 hepatocellular carcinoma cells were grown in DMEM medium containing 10% fetal bovine serum, 100 units/ml penicillin and 100 g/ml streptomycin. Human umbilical vein endothelial cells (HUVEC) were cultured in EBM-2 medium with endothelial cell growth supplement (Lonza, Hopkinton, MA). Proliferation was assessed by the XTT-based in vitro assay kit (Cayman, Ann Arbor, MI). To assess uptake of NPs, MCF-7 cells were seeded on coverslips and grown for 24 h. After incubation with Rhodamine B loaded NPs, the coverslips were removed, washed with PBS and fixed with 4% paraformaldehyde. The cells were then stained with DAPI and visualized under a confocal laser scanning microscope (CLSM, Olympus, Fluoview FV1000 Microscope, Japan).

Assessment of apoptosis

Cells were stained using the annexin V-alexa fluor 488/PI apoptosis assay kit (Invitrogen, Grand Island, NY). Quantification of apoptosis/necrosis was performed using Cellometer Vision (Nexcelom Bioscience LLC, Lawrence, MA). Cells were also imaged using the CLSM microsocope.

NIH-PA Author Manuscript

NIH-PA Author Manuscript

NIH-PA Author Manuscript

Immunoblot analysis

Cell lysates were prepared with M-PER reagent (Pierce Chemicals) and analyzed by immunoblotting with anti-BCL-2, anti-caspase-3 (Santa Cruz Biotechnology, Santa Cruz, CA) and anti-β-actin (Sigma, St. Louis, MO).

Analysis of anti-tumor activity

Mouse Ehrlich tumor cells were injected subcutaneously in the hind limb of syngeneic Balb/c mice (17-22 gms). Mice bearing tumors (~400 mm^3) were divided into 9 groups (10 mice/group) and treated intraperitoneally (IP) or intratumorally (IT) with different agents using two schedules for 21 d (Supplemental Table 1). Tumor volume was determined by calipers and calculated using the formula $(A \times B^2) \times 0.5$, where A and B are the longest and shortest tumor diameters, respectively. From each group, one mouse was sacrificed on day 7, 14 and 21 for harvesting of tumor for histopathologic examination. Statistical analysis of tumor volumes was performed by one-way ANOVA and the Dunnett test using Origin 8.0 (Origin Lab, Northampton, MA). Survival of the mice was determined by the Kaplan-Meier method using Prism 4.0 software (Graph Pad Software, Dan Diego, CA). One mouse from each of the control and NuBCP-9/NP-treated (IP once/week) groups was sacrificed on day 14 for tumor excision. The tumors were fixed in 10% formalin/saline and embedded in paraffin. Five-micron sections were stained with H&E.

Results

Preparation and characterization of NuBCP-9-loaded polymeric NPs

PLAPEG NPs have been commonly synthesized using PLA of ~20 kDa or less (19-21). In the present work, we studied the development of polymeric NPs that incorporate PLA of ~72 kDa to regulate the release of peptide drugs. PLAPEG and PLA-PEG-PPG-PEG block copolymers were synthesized by the DCC/DMAP conjugation method. As determined by GPC, the molecular weight of PLA was 72,487 daltons and it increased directly upon conjugation with increasing block length of PEG (1, 2 or 4 kDa) or with PEG-PPG-PEG (Table 1).[1] HNMR of PLA^{72K}-PEG showed peaks at 5.2 ppm ($OC\underline{H}(CH_3)C(O)_n$-O-$(CH_2CH_2O)_m$), 3.7 ppm ($OCH(CH_3)C(O)_n$-O-($\underline{CH_2CH_2}O)_m$), and 1.6 ppm ($OCH(\underline{CH_3})C(O)_n$-O-$(CH_2CH_2O)_m$). An additional peak at 2.1 ppm was observed for PLA^{72K}-PEG-PPG-PEG due to the – OCH_3 proton of PPG. These results confirmed coupling of PLA^{72K} with PEG or PEG-PPG-PEG.

The PLA-PEG block copolymer consists of a bilayer structure with the PLA hydrophobic core and the PEG hydrophilic shell interfacing with the aqueous medium. By contrast, conjugation of PEG-PPG-PEG with PLA results in multilayered NPs as a result of PPG extending the hydrophobic structure (22). SEM studies of both the PLA^{72K}-PEG^{4K} and PLA^{72K}-PEG-PPG-PEG NPs showed that the particles are spherical with uniform sizes ranging from 40-50 nm in diameter (Fig. 1A, left and right). The NPs were then loaded with Rhodamine B to assess their uptake in cells. Incubation of the Rhodamine B/PLA^{72K}-PEG^{4K} NPs with MCF-7 breast cancer cells demonstrated uptake over 3 to 12 h (Fig. 1B). The results further showed intracellular fluorescence of the Rhodamine B-NPs diffusely throughout the cytosol (Fig. 1B). Similar results were obtained with the Rhodamine B/

NIH-PA Author Manuscript

NIH-PA Author Manuscript

NIH-PA Author Manuscript

PLA^{72K}-PEG-PPG-PEG NPs (data not shown). Uptake of PLA-based NPs is through endocytosis and is associated with surface charge reversal (anionic to cationic) in the acidic pH of the endolysosomes. This charge reversal facilitates interaction of the NPs with vesicular membranes, leading to transient and localized membrane destabilization, and thereby escape of the NPs into the cytosol (23). Alternatively, Rhodamine B may have been released from the NPs. However, extensive washing of the NPs after Rhodamine B loading and the short 12 h duration of the experiment support a mechanism other than release.

Our results further demonstrate that the hydrophilic PEG segment of the block copolymers facilitated the encapsulation of the L-amino acid NuBCP-9 peptide into the core of the PLA^{72K}-PEG and PLA^{72K}-PEG-PPG-PEG NPs. For example, when the feeding ratio of NuBCP-9/block copolymers (w/w) was 1:10, the encapsulation efficiency of the different polymeric NPs ranged from 43% to 66% (Table 1). The encapsulation efficiency of NuBCP-9 in PLA^{72K}-PEG NPs was higher than that obtained with PLA^{72K} NPs (Table 1). In concert with those findings, increases in PEG chain length resulted in improved encapsulation of the hydrophilic NuBCP-9 peptide (Table 1) and maximum encapsulation was obtained with PLA^{72K}-PEG^{4K}. Moreover, the encapsulation efficiency of the PLA^{72K}-PEG-PPG-PEG NPs (64%) was similar to that obtained with the PLA^{72K}-PEG^{4K} NPs (66%) (Table 1). Final loading of NuBCP-9 into these PLA-based NPs was approximately 0.065 mg peptide/mg polymer and this concentration was used throughout the following in vitro and in vivo studies.

NTA measurements of the NPs documented a hydrodynamic diameter ranging from 114 to 125 nm, which did not change significantly after NuBCP-9 loading (Table 1). In addition, the hydrodynamic diameter of the NPs was not significantly altered by coupling to the different PEG molecular weights (1, 2 and 4 kDa), consistent with the greater mass of PLA as compared to PEG (Table 1). By contrast, the zeta potential of the NPs increased with increasing PEG block length (Table 1), a finding in concert with the demonstration that the zeta potential of NPs approaches neutral with increases in hydrophilicity due to PEG coupling (24). Notably, the zeta potential of the PLA^{72K}-PEG^{4K} NPs was similar to that for PLA^{72K}-PEG-PPG-PEG NPs before and after NuBCP-9 loading (Table 1). We also found that NuBCP-9 loading is associated with a marked decrease in zeta potential as compared to that obtained with the unloaded NPs (Table 1). The precise reason for this decrease in zeta potential is not clear; however, it is plausible that due to the interaction of the positively charged adsorbed peptide with the negatively charged PLA, the peptide carboxyl groups, which have a negative charge, are exposed on the surface of the nanoparticles. Studies have shown that negatively charged NPs are taken up less efficiently by cells in vitro as compared to positively charged NPs (25). However, negatively charged NPs are not cleared as rapidly from the circulation as positively charges NPs (25). Thus, the decrease in zeta potential of the NuBCP-9-loaded NPs could affect their behavior in vitro and in vivo.

Release of NuBCP-9 from NPs in vitro

The release profiles (percent cumulative release and percent release/day) of NuBCP-9 from the NPs was assessed at pH 7.4 over 60 d (Figs. 2A-D and Supplemental Figs. S1A-D). PLA^{72K} and PLA^{72K}-PEG NPs with PEG chain lengths of 1, 2 and 4 kDa exhibited

NIH-PA Author Manuscript

NIH-PA Author Manuscript

NIH-PA Author Manuscript

cumulative releases of 62%, 78%, 85% and 92%, respectively (Figs. 2A,B and Supplemental Figs. S1A and B). Maximum NuBCP-9 release at pH 7.4 was thus observed with the PLA^{72K}-PEG^{4K} NPs, consistent with an increase in flexibility and hydrophilicity, and thereby hydration of the NPs with increases in PEG chain length. At pH 5.0, the initial release of NuBCP-9 from PLA^{72K}-PEG NPs was similar to that found at pH 7.4 (Supplemental Figs. S2A and B). However, NuBCP-9 release at pH 5.0 was slower after day 7 and was only 68% as compared to 92% at pH 7.4 (Supplemental Figs. S2A and B). At pH 5.0, PLA chains remain in a coiled state and are thereby less susceptible to hydrolytic degradation (26, 27). By contrast, at pH 7.4, the PLA chains uncoil due to ionization, which is associated with an increase in NP degradation and release of NuBCP-9. The slower release at pH 5.0 could be a favorable characteristic in that there would be less NuBCP-9 release in the lysosome, a compartment with acidic pH, and thereby less degradation of the peptide. In addition, as compared to PLA^{72K}-PEG^{4K} NPs, release of NuBCP-9 from PLA^{72K}-PEG-PPG-PEG NPs was slower at pH 7.4 (Figs. 2A-D), which is likely due to the hydrophobic nature of the PPG in the PEG-PPG-PEG block. In this regard, the recent synthesis of PLA-PEG-PPG-PEG copolymers by ring opening polymerization of L-lactide has demonstrated that the hydrophilichydrophobic balance is not sufficient for the formation of bilayer vesicles and that the assembly of an onion-like vesicle is responsible for sustained insulin release (22).

Lower molecular weight PLA (12 kDa) was also used to synthesize PLA-PEG block copolymers to assess the effect on NuBCP-9 loading and release. The encapsulation efficiency of NuBCP-9 into PLA^{12K}-PEG-PPG-PEG was similar to that obtained with PLA^{72K}-PEG-PPG-PEG (Table 1). However, release of NuBCP-9 from PLA^{12K}-PEG-PPG-PEG was sustained for only 10 days as compared to 60 days for PLA^{72K}-PEG-PPG-PEG. After 10 days, peptide was no longer detectable in the filtrate, a finding probably due in part to the degradation and biosolubilization of low molecular weight PLA, which interferes with peptide detection in the assays (Figs. 2A-D). Based on these results, the NuBCP-9-encapsulated PLA^{72K}-PEG^{4K} and PLA^{72K}-PEG-PPG-PEG NPs were further studied for biologic activity *in vitro* and *in vivo*.

Effects of NuBCP-9-encapsulated NPs on cancer cell growth and survival in vitro

To assess activity of the NuBCP-9-loaded NPs, we studied their effects on growth of BCL-2-expressing MCF-7 (28) and HepG2 (29) cells and, as a control, primary HUVEC cells. Notably, NuBCP-9 is ineffective in inhibiting cancer cell proliferation in the absence of a CPP, such as r8 (6), and these observations were confirmed when NuBCP-9 was tested against MCF-7 and HepG2 cells (Figs. 3A and B). However, as expected from previous studies (6), the L-amino acid NuBCP-9-R8 (R denotes L-amino acid; r denotes D-amino) completely blocked growth of these cells after treatment at 15 μM for 48 h (Figs. 3A and B), confirming that R8 is necessary for cell penetration and BCL-2 targeting. Notably, the NuBCP-9 that has been encapsulated in NPs in the present studies is devoid of R8 and therefore would be expected to be inactive unless effectively delivered by the NPs. Indeed, the NuBCP-9-encapsulated NPs were highly effective in inhibiting growth of MCF-7 and HepG2 cells (Figs. 3A and B). By contrast, empty NPs not encapsulated with NuBCP-9 had little if any effect on growth (data not shown). Other studies were performed to assess the

NIH-PA Author Manuscript

NIH-PA Author Manuscript

NIH-PA Author Manuscript

effects of using different concentrations of NuBCP-9 NPs on cell viability. As expected, NuBCP-9-R8 induced death of MCF-7 cells in a concentration-dependent manner (Fig. 3C). In addition, the NuBCP-9 NPs (PLA^{72K}-PEG^{4K} and PLA^{72K}-PEG-PPG-PEG) were effective in killing MCF-7 cells (Fig. 3C). Similar results were obtained when HepG2 cells were treated with different concentrations of PLAPEG NPs (Fig. 3D). The IC_{50} values for the NuBCP-9 NPs ranged from 1.9 to 4.2 μM, as compared to 7.1 to 9.1 μM for NuBCP-9 R8 (Table 2). In addition and in concert with the lack of NuBCP-9 activity against normal cells (6), NuBCP-9-encapsulated NPs had no apparent effect on HUVEC cell growth (Fig. 3E). These results indicate that NuBCP-9 can be delivered intracellularly in an active form by polymeric NPs.

NuBCP-9/NPs induce apoptosis of cancer cells

NuBCP-9-r8 is a selective inducer of cancer cell apoptosis by targeting Bcl-2 (6). To assess the effects of NuBCP-9 NPs on the apoptotic response, MCF-7 cells were treated with NuBCP-9/PLA^{72K}-PEG^{4K} NPs and monitored for externalization of phosphatidylserine (PS) at the cell membrane. Confocal images of MCF-7 cells stained with Annexin V-Alexaflour 488/PI demonstrated that treatment with NuBCP-9 NPs is associated with the induction of an apoptotic response (Fig. 4A). By contrast, treatment with empty NPs had no apparent effect (Fig. 4A). Quantitation of annexin V and PI staining by flow cytometry confirmed that NuBCP-9 PLA^{72K}-PEG^{4K} NPs and NuBCP-9 PLA^{72K}-PEG-PPG-PEG NPs are as effective as NuBCP-9-R8 in inducing apoptosis of MCF-7 cells at 48 h (Fig. 4B). As controls, empty PLA^{72K}-PEG^{4K} NPs and NuBCP-9 devoid of R8 had little, if any effect on MCF-7 cell apoptosis (Fig. 4B). As reported (28, 29), immunoblot analysis of MCF-7 and HepG2 cell lysates confirmed the expression of BCL-2 (Fig. 4C). Moreover and in concert with the effects of NuBCP-9 on BCL-2 (6), treatment of MCF-7 and HepG2 cells with NuBCP-9 NPs was associated with activation of caspase-3 (Fig. 4D). These findings thus demonstrate that, like NuBCP-9-R8, encapsulation of NuBCP-9 in NPs results in the induction of apoptosis (Fig. 4D).

NuBCP-9-NPs are effective in inducing complete tumor regressions

To assess the anti-tumor effects of NuBCP-9 NPs in vivo, we treated Balb/c mice bearing established (~400 mm^3) subcutaneous BCL-2-positive Ehrlich syngeneic tumors (30). In this widely used model to assess the effects of anti-cancer agents, accurate administration of the viscous suspensions of NPs was problematic in the narrow tail vein. As such, we used the intraperitoneal (IP) route of administration, which allows NPs to enter the systemic circulation through mesenteric vessels and the portal vein (31). Moreover, these studies were performed with NuBCP-9 (devoid of R8) because (i) NuBCP-9-R8 is active in vivo when administered intratumorally (6), and (ii) the NuBCP-9 should be inactive in the absence of a CPP. IP injection of NuBCP-9 on a twice weekly schedule for 21 days had no significant effect on tumor growth as compared to that obtained with the saline control (PBS) (Fig. 5A and Supplemental Table 1). Significantly, IP treatment with NuBCP-9 $PLA^{72K}PEG^{4K}$ NPs at a dose of 20 mg/kg (NuBCP-9 peptide dose) on the same schedule was associated with complete and prolonged tumor regressions (Fig. 5A). Moreover, in contrast to the empty PLA^{72K}-PEG^{4K} NPs, IP injection of NuBCP-9 PLA^{72K}-PEG^{4K} NPs on a weekly schedule for 21 days resulted in similar anti-tumor responses (Fig. 5B). For assessment of direct

NIH-PA Author Manuscript

NIH-PA Author Manuscript

NIH-PA Author Manuscript

delivery of NuBCP-9 NPs into the tumors, we also administered NuBCP-9 PLA^{72K}-PEG-PPG-PEG NPs intratumorally (IT) on a twice weekly schedule for 21 days and compared the effects of IP administration of PLA^{72K}-PEG-PPG-PEG on tumor growth. The results demonstrate that regression of the tumors was similar when the NuBCP-9 NPs were delivered IT as compared to IP (Fig. 5C). However, IP treatment was more effective than IT in maintaining these anti-tumor responses after completing treatment (Fig. 5C). Similar results were obtained when NuBCP-9 PLA^{72K}-PEG^{4K} NPs were administered IT weekly or twice weekly (Supplementary Fig S3). Analysis of survival as determined by Kaplan-Meier plots further demonstrated that mice treated with NuBCP-9 NPs (PLA^{72K}-PEG^{4K} or PLA^{72K}-PEG-PPG-PEG) weekly or twice weekly survived significantly longer than the saline, empty NPs or NuBCP-9 controls (Fig. 5D and E). Moreover, the NuBCP-9 NPs-treated mice survived longer when administration was IP as compared to the IT route (Fig. 5D and E). Significantly, there was no weight loss or other overt toxicities observed in the NuBCP-9/NP-treated mice (data not shown). Analysis of tissue sections demonstrated that tumor cells from the control mice exhibited mitosis and little, if any, evidence of necrosis (Fig. 5F, left). By contrast, tumor cells from NuBCP-9 PLA^{72K}-PEG^{4K} NPs-treated mice had decreased mitotic activity and considerably larger regions of necrosis (Fig. 5F, right), consistent with the anti-tumor activity of NuBCP-9.

Discussion

Peptide drugs have considerable potential for targeting intracellular oncoproteins that lack hydrophobic pockets and are thereby not eminently druggable with small molecules (32). In this context, there are increasing reports of peptide drugs under development that target non-kinase proteins such as survivin (33), HDM2 (34), NOTCH (35), MUC1 (36) and β-catenin (37), among others. The BCL-2 family proteins have also been the focus of peptide inhibitor development, specifically in one strategy using stabilized alpha-helices of BCL-2 domains (SAHBs) (38). BCL-2 has also been converted from an anti-apoptotic protein to an inducer of cell death by the Nur77-derived NuBCP peptide (6, 7). With the exception of SAHBs, which penetrate cell membranes, delivery of peptide drugs has in general required the addition of a PTD for intracellular delivery (11). In this way, NuBCP was linked to the CPP D-Arg octamer (r8) (6). NuBCP-9-r8 is a potent and selective inducer of cancer cell apoptosis in vitro (6). NuBCP-9-r8 is also effective in inducing apoptosis in vivo when injected directly into tumors (6). Indeed, a challenge for the development of many peptide drugs, like NuBCP-9, is the potential for systemic delivery, which can be limited by pharmacologic parameters, such as short circulating half-lives, that prevent prolonged drug exposure. For example, systemic delivery of MUC1-targeted peptides has necessitated frequent daily dosing for effective anti-tumor activity in xenograft tumor models (36). The present studies, using NuBCP-9 as a model, were therefore performed to assess the delivery and release of an anti-cancer peptide drug in NPs.

NPs are being widely used for the effective delivery of small molecules (19-21). However, the collective experience with encapsulation of peptides into NPs is limited. A polycationic peptide targeting BCL-2 has been incorporated into cationic liposomes as a potential anticancer agent (39, 40). In addition, the membrane-disrupting cytolytic peptide, melittin, has been incorporated into the outer lipid monolayer of a perfluorocarbon nanoemulsion

NIH-PA Author Manuscript

NIH-PA Author Manuscript

NIH-PA Author Manuscript

vehicle to target tumors (41). Other cytoxic peptides have been developed in cyclodextrin polymerized NPs, glycolide NPs and poly(propylacrylic acid) NPs (42, 43). To our knowledge, none of these peptide nanoformulations have been further developed for clinical evaluation. In this context, a significant consideration for the clinical development of NPs is the concentration of emulsifier, which at high levels can be toxic to kidneys. In the present studies, the PLA-PEG and PLA-PEGPPG-PEG NPs were prepared using a double emulsion solvent evaporation method (44). Our results show that an advantage of using PEG-PPG-PEG as a block copolymer in preparation of PLA NPs is that emulsifier concentrations can be markedly reduced for PLA NP stabilization at pH 7.4. Indeed, for PLA-PEG NPs, the final emulsifier concentration was 0.4%, however, we were able to further reduce that concentration by 5-fold to 0.08% for the PLA-PEG-PPG-PEG NPs. These findings are therefore of potential significance for the clinical development of these polymeric NPs.

Based on the results obtained with our double emulsion method, we studied loading of NuBCP-9 in the PLA-PEG and PLA-PEG-PPG-PEG NPs. Previous work had demonstrated that increasing PEG chain length from 1 to 4 kDa significantly improves the hydrophilicity and flexibility of block copolymers (44). Consequently, we analyzed the effects of different lengths of the PEG block and found that increases in PEG chain length improves NuBCP-9 loading. Moreover, our results demonstrate that release of NuBCP-9 over time is enhanced by increases in PEG chain length, a finding in concert with greater flexibility, hydrophilicity and hydration of the NP. In turn, the rate of diffusion increases, as does release of the peptide from the NP matrix (20, 45-48). Thus, for NuBCP-9 and potentially other peptide drugs, these findings indicate that PEG chain length is of importance for both loading in and release from polymeric NPs. Another aspect of our studies worth highlighting is the use of a high molecular weight PLA (72 kDa) in the NuBCP-9 encapsulated NPs. Previous work on polymeric NPs has generally involved lower molecular weight PLA, for example, using 20 kDa or less (49, 50). Our results indicate that in vitro release of NuBCP-9 from our NPs was sustained to over 60 d when using ~72 kDa PLA as compared to release of the peptide over 10 d with ~12 kDa PLA. These results can be explained, at least in part, by the hydrolysis of PLA and thereby NuBCP-9 diffusion. At pH 5.0, PLA remains coiled and is less susceptible to hydrolysis; whereas at pH 7.4, the PLA chains open with an increased propensity for hydrolysis. The uncoiling of PLA is thus associated with an increase in its degradation and release of NuBCP-9 (26, 27). These findings collectively indicate that peptide release from polymeric NPs can be controlled by varying the sizes of the PEG and PLA blocks.

NuBCP-9 is a highly promising anti-cancer peptide that selectively induces apoptosis of cancer cells by exposing the BCL-2 BH3 domain and blocking the BCL-xL survival function (6). NuBCP-9 was linked to the D-Arg octamer r8 for intracellular delivery, a modification that has been reported to decrease selectivity by inducing BCL-2-independent cell killing involving membrane disruption (15). In the present work, delivery of NuBCP-9 into cancer cells by the polymeric NPs was achieved without the need for the R8 PTD. In addition, the NuBCP-9 encapsulated NPs were by comparison more potent in inducing apoptosis than NuBCP-9-R8. The NuBCP-9/NPs also maintained the reported selectivity of NuBCP-9 for cancer cells as evidenced by their absence of HUVEC killing (6). Previous studies of the anti-tumor effects of NuBCP-9 in vivo were performed by direct injection of NuBCP-9-r8 into MDA-MB-435 breast cancer xenografts growing in SCID mice (6). Under

NIH-PA Author Manuscript

NIH-PA Author Manuscript

NIH-PA Author Manuscript

these experimental conditions, NuBCP-9-r8 treatment was associated with partial MDA-MB-435 tumor regressions (6). In the present studies using the subcutaneous Ehrlich tumor model in syngeneic mice, we compared the effectiveness of NuBCP-9/NPs administered intraperitoneally (IP) and intratumorally (IT). Significantly, both routes of NuBCP-9/NP administration were effective in inducing complete regressions of the Ehrlich tumors. Moreover and interestingly, IP administration was more effective than IT delivery in maintaining prolonged tumor regressions. The basis for this distinction is presently not clear, but is likely related to pharmacokinetics and pharmacodynamics of the NuBCP-9/NPs, which will be the focus of subsequent studies. Of further importance, administration of the NuBCP-9/NPs was well-tolerated with no evidence of weight loss or overt toxicities. These results thus provide support for the effective delivery of L-amino acid NuBCP-9 by PLA-PEG-PPG-PEG NPs and may be applicable to other anti-cancer peptides. In summary, our findings describe a novel NP-based approach for delivery of L-amino acid peptides without a cell-penetrating domain that (i) requires reduced levels of emulsifier, (ii) incorporates higher molecular weights of PLA for sustained and prolonged peptide release, (iii) induces effective anti-cancer activity in vitro and in vivo, and (iv) requires less frequent dosing (once/week) compared to the daily injections that were necessary for partial anti-tumor activity of the D-amino acid NuBCP-9-r8 peptide in vivo (6).

Supplementary Material

Refer to Web version on PubMed Central for supplementary material.

Acknowledgments

Grant Support

Research reported in this publication was supported by the National Cancer Institute of the National Institutes of Health under award number CA97098, by the Lung Cancer Research Foundation, and by a grant from the Department of Science and Technology, Government of India.

Abbreviations

NP	nanoparticle
PEG	polyethylene glycol
PLA	polylactic acid
PPG	polypropylene glycol
MOMP	mitochondrial outer membrane potential
BH	BCL-2 homology
PTD	protein transduction domain
CPP	cell-penetrating peptide
DCC	N,N-dicyclohexylcarbodimide
DMAP	4-dimethylaminopyridine

NIH-PA Author Manuscript

NIH-PA Author Manuscript

NIH-PA Author Manuscript

GPC gel permeation chromatography

References

1. Cory S, Huang DC, Adams JM. The Bcl-2 family: roles in cell survival and oncogenesis. Oncogene. 2003; 22:8590–607. [PubMed: 14634621]
2. Green DR, Kroemer G. The pathophysiology of mitochondrial cell death. Science. 2004; 305:626–9. [PubMed: 15286356]
3. Pitter K, Bernal F, Labelle J, Walensky LD. Dissection of the BCL-2 family signaling network with stabilized alpha-helices of BCL-2 domains. Methods Enzymol. 2008; 446:387–408. [PubMed: 18603135]
4. Oltersdorf T, Elmore SW, Shoemaker AR, Armstrong RC, Augeri DJ, Belli BA, et al. An inhibitor of Bcl-2 family proteins induces regression of solid tumours. Nature. 2005; 435:677–81. [PubMed: 15902208]
5. Tse C, Shoemaker AR, Adickes J, Anderson MG, Chen J, Jin S, et al. ABT-263: a potent and orally bioavailable Bcl-2 family inhibitor. Cancer Res. 2008; 68:3421–8. [PubMed: 18451170]
6. Kolluri SK, Zhu X, Zhou X, Lin B, Chen Y, Sun K, et al. A short Nur77-derived peptide converts Bcl-2 from a protector to a killer. Cancer Cell. 2008; 14:285–98. [PubMed: 18835031]
7. Lin B, Kolluri SK, Lin F, Liu W, Han YH, Cao X, et al. Conversion of Bcl-2 from protector to killer by interaction with nuclear orphan receptor Nur77/TR3. Cell. 2004; 116:527–40. [PubMed: 14980220]
8. Bidwell GL 3rd, Raucher D. Therapeutic peptides for cancer therapy. Part I - peptide inhibitors of signal transduction cascades. Expert Opin Drug Deliv. 2009; 6:1033–47. [PubMed: 19637980]
9. Raucher D, Moktan S, Massodi I, Bidwell GL 3rd. Therapeutic peptides for cancer therapy. Part II - cell cycle inhibitory peptides and apoptosis-inducing peptides. Expert Opin Drug Deliv. 2009; 6:1049–64. [PubMed: 19743895]
10. Talmadge JE. Pharmacodynamic aspects of peptide administration biological response modifiers. Adv Drug Deliv Rev. 1998; 33:241–52. [PubMed: 10837664]
11. Fischer PM. Cellular uptake mechanisms and potential therapeutic utility of peptidic cell delivery vectors: progress 2001-2006. Med Res Rev. 2007; 27:755–95. [PubMed: 17019680]
12. Grdisa M. The delivery of biologically active (therapeutic) peptides and proteins into cells. Curr Med Chem. 2011; 18:1373–9. [PubMed: 21366527]
13. Li H, Nelson CE, Evans BC, Duvall CL. Delivery of intracellular-acting biologics in pro-apoptotic therapies. Curr Pharm Des. 2011; 17:293–319. [PubMed: 21348831]
14. Gu Z, Biswas A, Zhao M, Tang Y. Tailoring nanocarriers for intracellular protein delivery. Chem Soc Rev. 2011; 40:3638–55. [PubMed: 21566806]
15. Watkins CL, Sayers EJ, Allender C, Barrow D, Fegan C, Brennan P, et al. Co-operative membrane disruption between cell-penetrating peptide and cargo: implications for the therapeutic use of the Bcl-2 converter peptide D-NuBCP-9-r8. Mol Ther. 2011; 19:2124–32. [PubMed: 21934653]
16. Kratz F, Warnecke A. Finding the optimal balance: challenges of improving conventional cancer chemotherapy using suitable combinations with nano-sized drug delivery systems. J Control Release. 2012; 164:221–35. [PubMed: 22705248]
17. Manzoor AA, Lindner LH, Landon CD, Park JY, Simnick AJ, Dreher MR, et al. Overcoming limitations in nanoparticle drug delivery: triggered, intravascular release to improve drug penetration into tumors. Cancer Res. 2012; 72:5566–75. [PubMed: 22952218]
18. Zhang XY, Chen J, Zheng YF, Gao XL, Kang Y, Liu JC, et al. Follicle-stimulating hormone peptide can facilitate paclitaxel nanoparticles to target ovarian carcinoma in vivo. Cancer Res. 2009; 69:6506–14. [PubMed: 19638590]
19. Kamaly N, Xiao Z, Valencia PM, Radovic-Moreno AF, Farokhzad OC. Targeted polymeric therapeutic nanoparticles: design, development and clinical translation. Chem Soc Rev. 2012; 41:2971–3010. [PubMed: 22388185]

NIH-PA Author Manuscript

NIH-PA Author Manuscript

NIH-PA Author Manuscript

20. Xiao RZ, Zeng ZW, Zhou GL, Wang JJ, Li FZ, Wang AM. Recent advances in PEG-PLA block copolymer nanoparticles. Int J Nanomedicine. 2010; 5:1057–65. [PubMed: 21170353]
21. Kim TY, Kim DW, Chung JY, Shin SG, Kim SC, Heo DS, et al. Phase I and pharmacokinetic study of Genexol-PM, a cremophor-free, polymeric micelle-formulated paclitaxel, in patients with advanced malignancies. Clin Cancer Res. 2004; 10:3708–16. [PubMed: 15173077]
22. Xiong XY, Li QH, Li YP, Guo L, Li ZL, Gong YC. Pluronic P85/poly(lactic acid) vesicles as novel carrier for oral insulin delivery. Colloids Surf B Biointerfaces. 2013; 111C:282–8. [PubMed: 23838194]
23. Panyam J, Zhou WZ, Prabha S, Sahoo SK, Labhasetwar V. Rapid endolysosomal escape of poly(DL-lactide-co-glycolide) nanoparticles: implications for drug and gene delivery. FASEB J. 2002; 16:1217–26. [PubMed: 12153989]
24. Doiron AL, Chu K, Ali A, Brannon-Peppas L. Preparation and initial characterization of biodegradable particles containing gadolinium-DTPA contrast agent for enhanced MRI. Proc Natl Acad Sci U S A. 2008; 105:17232–7. [PubMed: 18796605]
25. Albanese A, Tang PS, Chan WC. The effect of nanoparticle size, shape, and surface chemistry on biological systems. Annu Rev Biomed Eng. 2012; 14:1–16. [PubMed: 22524388]
26. Andersson SR, Hakkarainen M, Inkinen S, Sodergard A, Albertsson AC. Customizing the hydrolytic degradation rate of stereocomplex PLA through different PDLA architectures. Biomacromolecules. 2012; 13:1212–22. [PubMed: 22394150]
27. Hoglund A, Odelius K, Albertsson AC. Crucial differences in the hydrolytic degradation between industrial polylactide and laboratory-scale poly(L-lactide). ACS Appl Mater Interfaces. 2012; 4:2788–93. [PubMed: 22563747]
28. Nathan B, Gusterson B, Jadayel D, O'Hare M, Anbazhagan R, Jayatilake H, et al. Expression of BCL-2 in primary breast cancer and its correlation with tumour phenotype. For the International (Ludwig) Breast Cancer Study Group. Ann Oncol. 1994; 5:409–14. [PubMed: 7915536]
29. Tan J, Wang B, Zhu L. Regulation of survivin and Bcl-2 in HepG2 cell apoptosis induced by quercetin. Chem Biodivers. 2009; 6:1101–10. [PubMed: 19623560]
30. Bhattacharyya A, Choudhuri T, Pal S, Chattopadhyay S, G KD, Sa G, et al. Apoptogenic effects of black tea on Ehrlich's ascites carcinoma cell. Carcinogenesis. 2003; 24:75–80. [PubMed: 12538351]
31. Turner PV, Brabb T, Pekow C, Vasbinder MA. Administration of substances to laboratory animals: routes of administration and factors to consider. J Am Assoc Lab Anim Sci. 2011; 50:600–13. [PubMed: 22330705]
32. Verdine GL, Walensky LD. The challenge of drugging undruggable targets in cancer: lessons learned from targeting BCL-2 family members. Clin Cancer Res. 2007; 13:7264–70. [PubMed: 18094406]
33. Plescia J, Salz W, Xia F, Pennati M, Zaffaroni N, Daidone MG, et al. Rational design of shepherdin, a novel anticancer agent. Cancer Cell. 2005; 7:457–68. [PubMed: 15894266]
34. Sarafraz-Yazdi E, Bowne WB, Adler V, Sookraj KA, Wu V, Shteyler V, et al. Anticancer peptide PNC-27 adopts an HDM-2-binding conformation and kills cancer cells by binding to HDM-2 in their membranes. Proc Natl Acad Sci U S A. 2010; 107:1918–23. [PubMed: 20080680]
35. Moellering RE, Cornejo M, Davis TN, Del Bianco C, Aster JC, Blacklow SC, et al. Direct inhibition of the NOTCH transcription factor complex. Nature. 2009; 462:182–8. [PubMed: 19907488]
36. Raina D, Kosugi M, Ahmad R, Panchamoorthy G, Rajabi H, Alam M, et al. Dependence on the MUC1-C oncoprotein in non-small cell lung cancer cells. Mol Cancer Therapeutics. 2011; 10:806–16.
37. Grossmann TN, Yeh JT, Bowman BR, Chu Q, Moellering RE, Verdine GL. Inhibition of oncogenic Wnt signaling through direct targeting of beta-catenin. Proc Natl Acad Sci U S A. 2012; 109:17942–7. [PubMed: 23071338]
38. Stewart ML, Fire E, Keating AE, Walensky LD. The MCL-1 BH3 helix is an exclusive MCL-1 inhibitor and apoptosis sensitizer. Nat Chem Biol. 2010

NIH-PA Author Manuscript

NIH-PA Author Manuscript

NIH-PA Author Manuscript

39. Ko YT, Falcao C, Torchilin VP. Cationic liposomes loaded with proapoptotic peptide D-(KLAKLAK)(2) and Bcl-2 antisense oligodeoxynucleotide G3139 for enhanced anticancer therapy. Mol Pharm. 2009; 6:971–7. [PubMed: 19317442]
40. Adar L, Shamay Y, Journo G, A D. Pro-apoptic peptide-polymer conjugates to induce mitochondrial-dependent cell death. Polym Adv Technol. 2010; 22:199–208.
41. Soman NR, Baldwin SL, Hu G, Marsh JN, Lanza GM, Heuser J, et al. Molecularly targeted nanocarriers deliver the cytolytic peptide melittin specifically to tumor cells in mice, reducing cell growth. J Clin Invest. 2009; 119:2830–42. [PubMed: 19726870]
42. Schluep T, Gunawan P, Ma L, Jensen GS, Duringer J, Hinton S, et al. Polymeric tubulysin-peptide nanoparticles with potent antitumor activity. Clin Cancer Res. 2009; 15:181–9. [PubMed: 19118045]
43. Kim SK, Huang L. Nanoparticle delivery of a peptide targeting EGFR signaling. J Control Release. 2012; 157:279–86. [PubMed: 21871507]
44. Tomar L, Tyagi C, Kumar M, Kumar P, Singh H, Choonara YE, et al. In vivo evaluation of a conjugated poly(lactide-ethylene glycol) nanoparticle depot formulation for prolonged insulin delivery in the diabetic rabbit model. Int J Nanomedicine. 2013; 8:505–20. [PubMed: 23429428]
45. Essa S, Rabanel JM, Hildgen P. Effect of polyethylene glycol (PEG) chain organization on the physicochemical properties of poly(D, L-lactide) (PLA) based nanoparticles. Eur J Pharm Biopharm. 2010; 75:96–106. [PubMed: 20211727]
46. Feng R, Song Z, Zhai G. Preparation and in vivo pharmacokinetics of curcumin-loaded PCL-PEG-PCL triblock copolymeric nanoparticles. Int J Nanomedicine. 2012; 7:4089–98. [PubMed: 22888245]
47. Hans M, Lowman A. Biodegradable nanoparticles for drug delivery and targeting. Current Opinion in Solid State & Materials Science. 2002; 6:319–27.
48. Wang B, Jiang W, Yan H, Zhang X, Yang L, Deng L, et al. Novel PEG-graft-PLA nanoparticles with the potential for encapsulation and controlled release of hydrophobic and hydrophilic medications in aqueous medium. Int J Nanomedicine. 2011; 6:1443–51. [PubMed: 21796246]
49. Hrkach J, Von Hoff D, Mukkaram Ali M, Andrianova E, Auer J, Campbell T, et al. Preclinical development and clinical translation of a PSMA-targeted docetaxel nanoparticle with a differentiated pharmacological profile. Sci Transl Med. 2012; 4:128ra39.
50. Farokhzad OC, Cheng J, Teply BA, Sherifi I, Jon S, Kantoff PW, et al. Targeted nanoparticle-aptamer bioconjugates for cancer chemotherapy in vivo. Proc Natl Acad Sci U S A. 2006; 103:6315–20. [PubMed: 16606824]

NIH-PA Author Manuscript

NIH-PA Author Manuscript

NIH-PA Author Manuscript

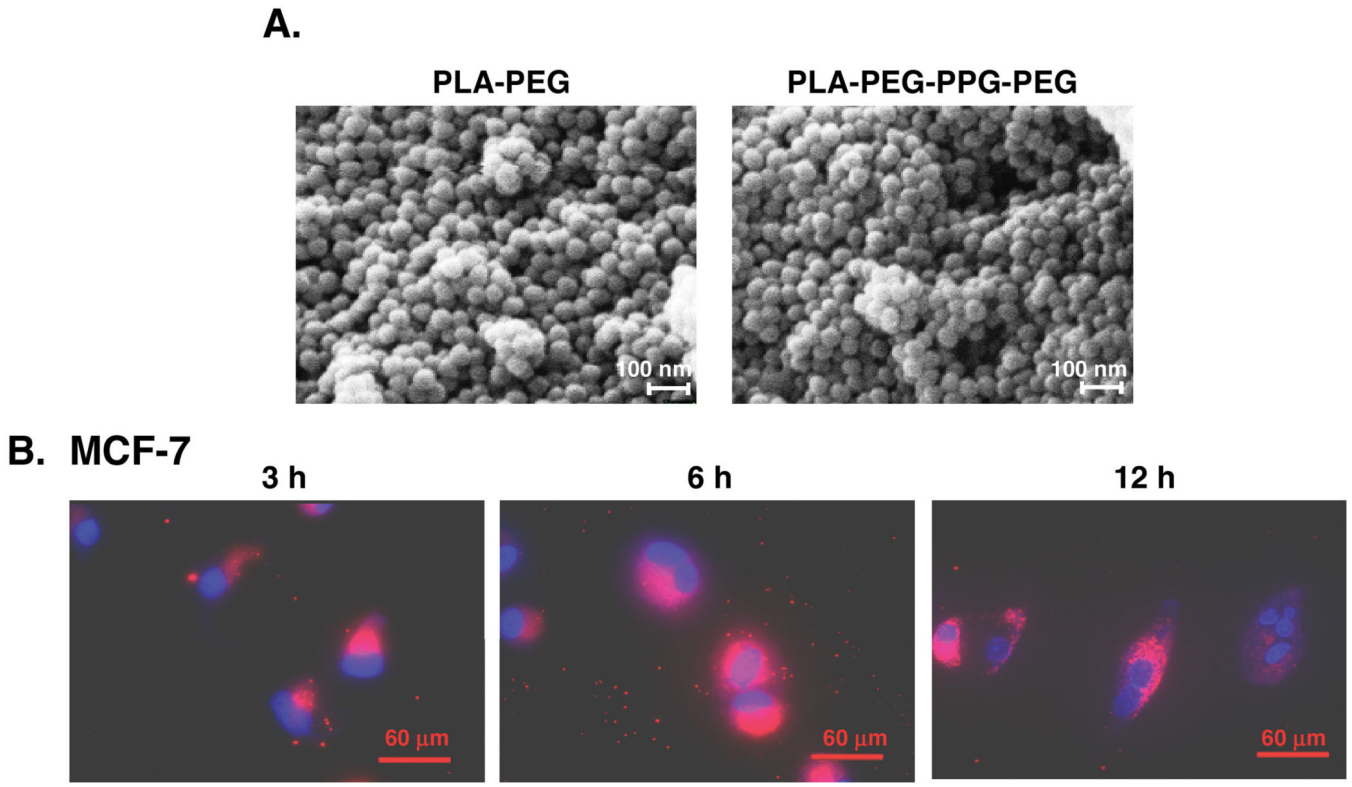

Figure 1. Cellular uptake of the PLA^{72K}-PEG NPs

A. Scanning electron micrographs (SEM) of the indicated PLA^{72K}-PEG^{4K} and PLA^{72K}-PEG-PPG-PEG NPs. Scales bars: 100 nm. B. PLA^{72K}-PEG^{4K} NPs were loaded with Rhodamine B and then incubated with MCF-7 cells for the indicated times. CLSM images are shown with detection of intracellular Rhodamine B (red) and DAPI staining of nuclei (blue). Scale bars: 60 μm.

NIH-PA Author Manuscript

NIH-PA Author Manuscript

NIH-PA Author Manuscript

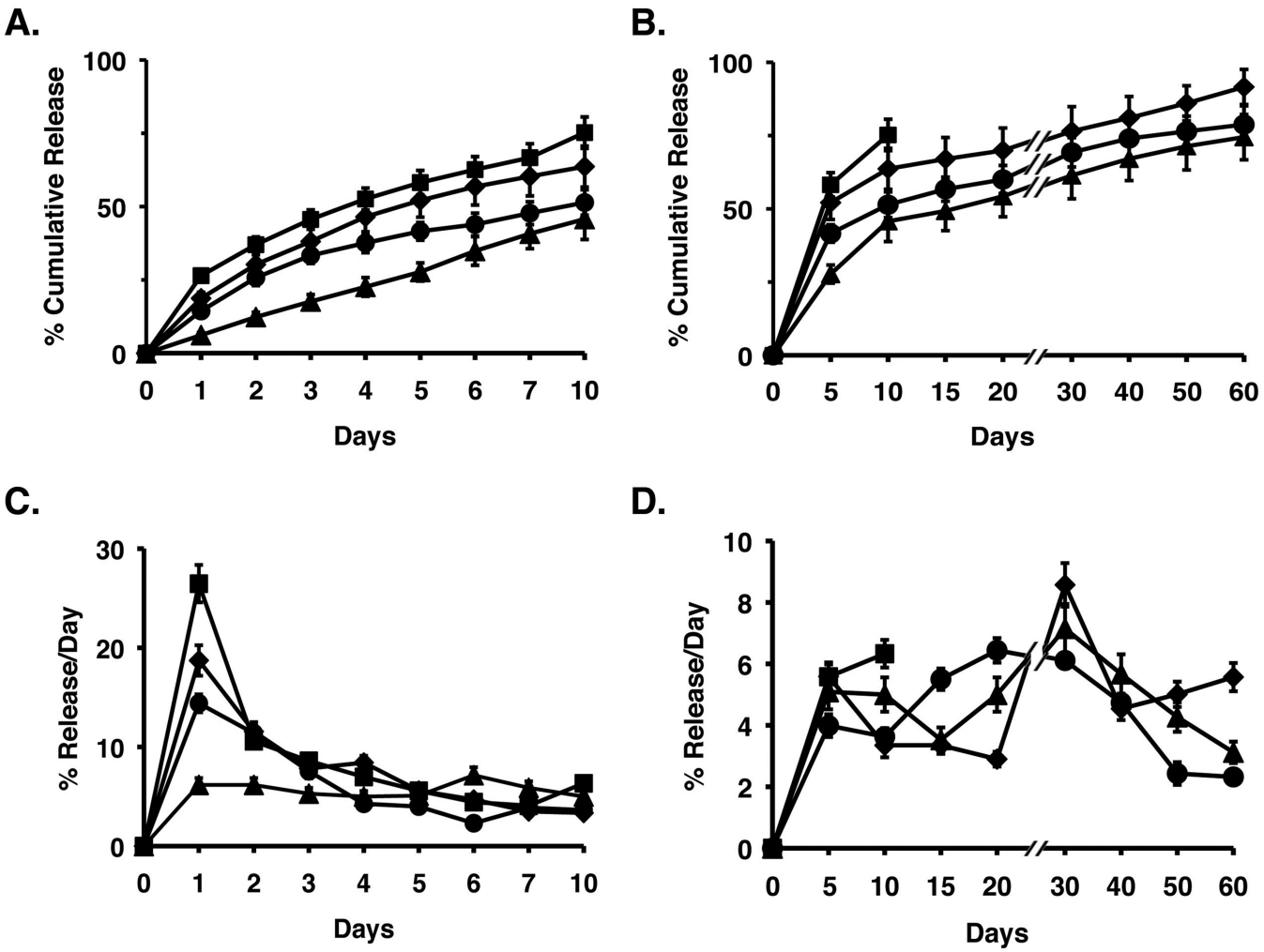

Figure 2. Release of NuBCP-9 from NPs

A and B. Percentage cumulative release studies of NuBCP-9 from PLA^{72K} (triangles), PLA^{72K}-PEG^{4K} (diamonds), PLA^{12K}-PEG-PPG-PEG (squares) and PLA^{72K}-PEG-PPG-PEG (circles) NPs in PBS at pH 7.4. Results are expressed as the mean+SD of three replicates. C and D. Percentage release of peptide/day studies of NuBCP-9 from PLA^{72K} (triangles), PLA^{72K}-PEG^{4K} (diamonds), PLA^{12K}-PEG-PPG-PEG (squares) and PLA^{72K}PEG-PPG-PEG (circles) NPs in PBS at pH 7.4. Results are expressed as the mean +SD of three replicates.

NIH-PA Author Manuscript

NIH-PA Author Manuscript

NIH-PA Author Manuscript

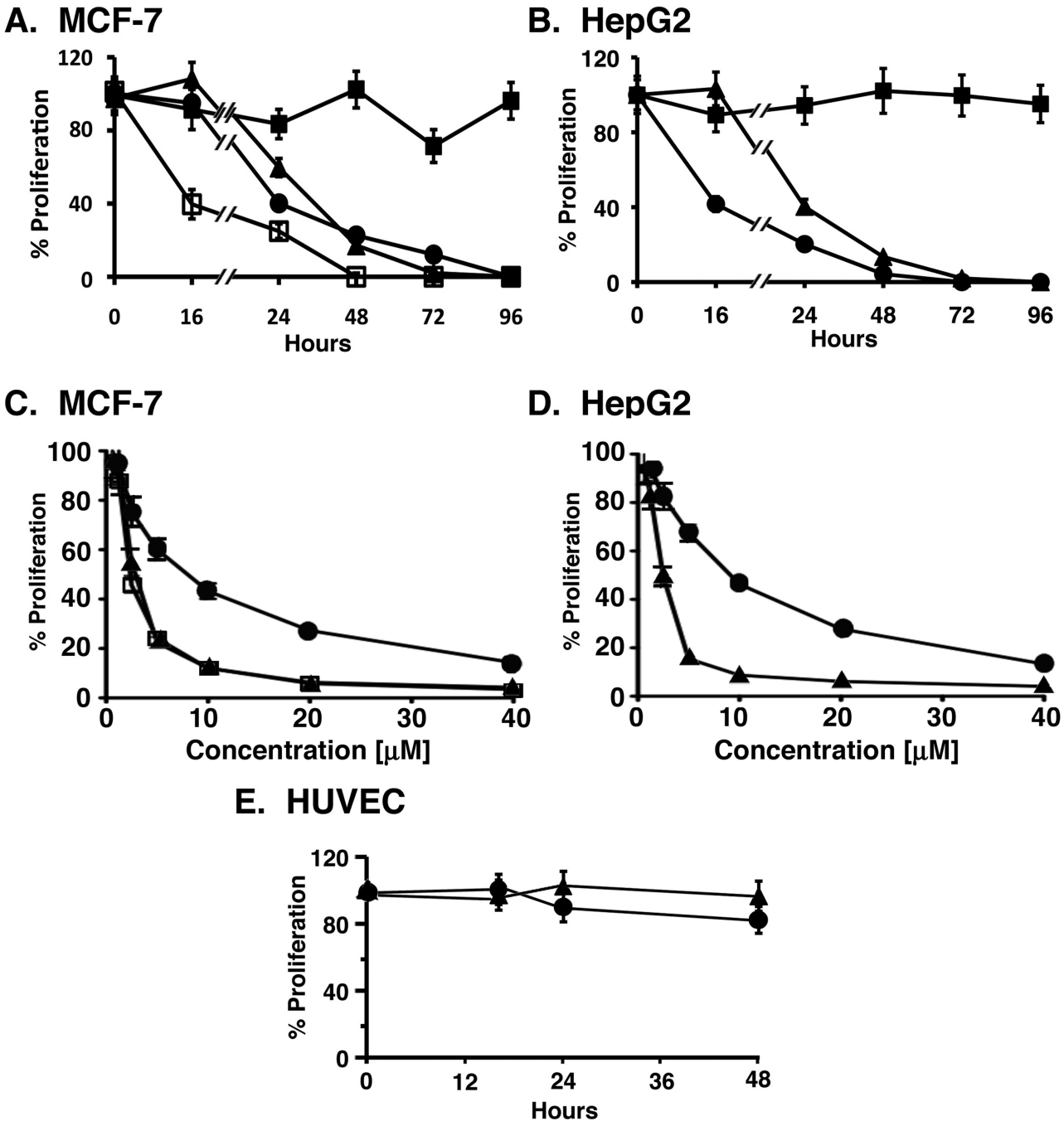

Figure 3. Effects of NuBCP-9 and NuBCP-9 NPs on carcinoma cell proliferation

A. MCF-7 breast carcinoma cells were treated with 15 μM NuBCP-9 (closed squares), 15 μM NuBCP-9-R8 (closed circles), NuBCP-9 $PLA^{72K}PEG^{4K}$ NPs (15 μM NuBCP-9 peptide; closed triangles) or NuBCP-9/PLA^{72K}-PEG-PPG PEG NPs (15 μM NuBCP-9 peptide; open squares) for the indicated times. Cell proliferation was assessed by XTT assays. Results are expressed as mean±SE of three independent experiments. B. HepG2 hepatocellular carcinoma cells were treated with 15 μM NuBCP-9 (closed squares), 15 μM NuBCP-9-R8 (closed circles) or NuBCP-9 PLA^{72K}-PEG^{4K} NPs (15 μM NuBCP-9 peptide; closed

NIH-PA Author Manuscript

NIH-PA Author Manuscript

NIH-PA Author Manuscript

triangles) for the indicated times. Cell proliferation was assessed by XTT assays. Results are expressed as mean±SE of three independent experiments. C. MCF-7 cells were treated with different NuBCP-9 concentrations [μM] of NuBCP-9-R8 (closed circles), NuBCP-9 PLA^{72K}-PEG^{4K} NPs (closed triangles) or NuBCP-9 PLA^{72K}-PEG-PPG-PEG NPs (open squares) for 72 h. Cell proliferation was assessed by XTT assays. Results are expressed as mean±SE of three independent experiments. D. HepG2 cells were treated with different NuBCP-9 concentrations [μM] of NuBCP-9-R8 (closed circles) or NuBCP-9 PLA^{72K}-PEG^{4K} NPs (closed triangles) for 72 h. Cell proliferation was assessed by XTT assays. Results are expressed as mean+SE of three independent experiments. E. HUVECs were treated with 15 μM NuBCP-9-R8 (closed circles) and NuBCP-9 PLA^{72K}-PEG^{4K} NPs (15 μM NuBCP-9 peptide; closed triangles) for the indicated times. Cell proliferation was assessed by XTT assays. Results are expressed as mean+SE of three independent experiments.

NIH-PA Author Manuscript

NIH-PA Author Manuscript

NIH-PA Author Manuscript

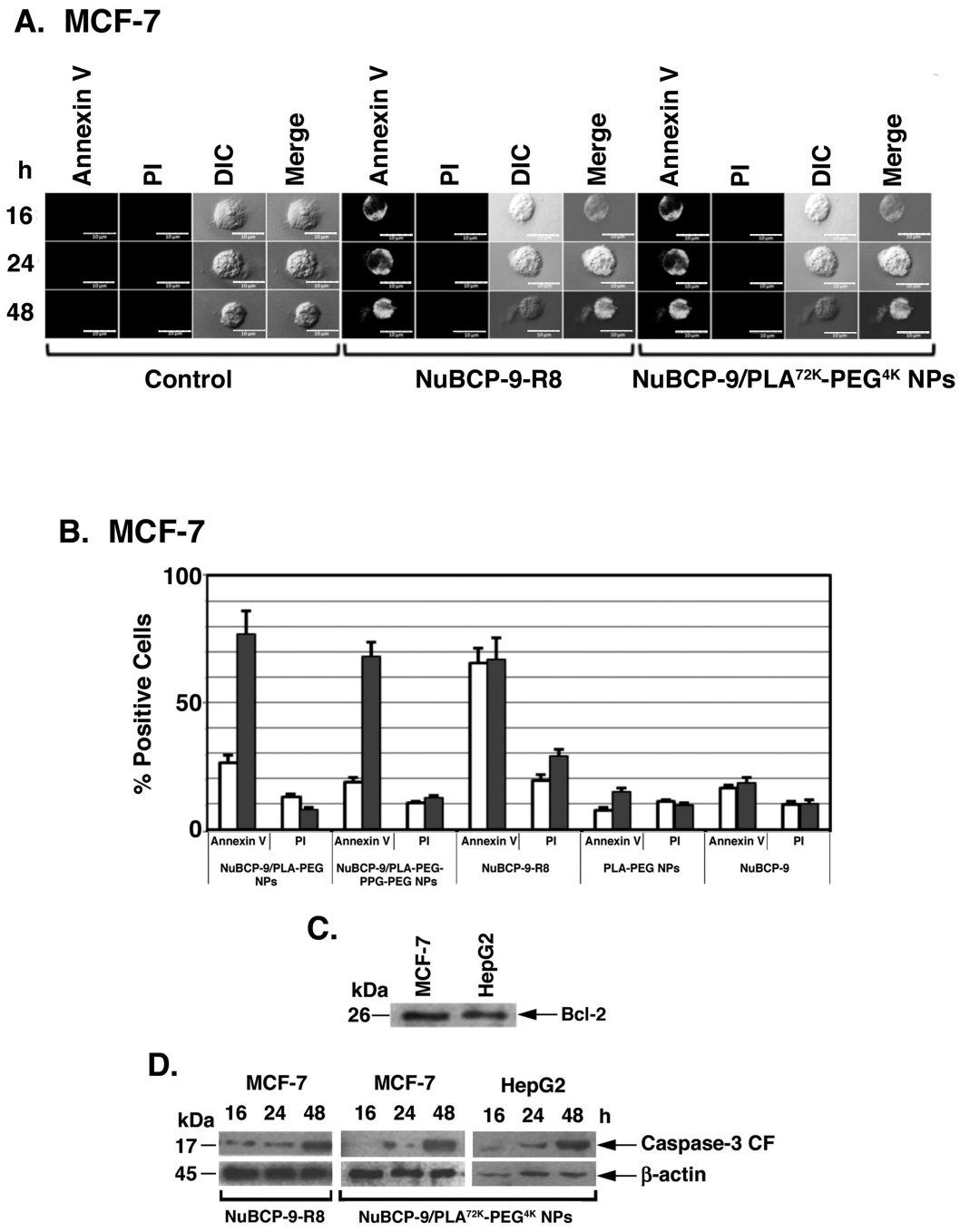

Figure 4. Effects of NuBCP-9-R8 and NuBCP-9/NPs on induction of cell death

A. Confocal laser scanning microscopic images of Annexin V/PI double staining of MCF-7 cells left untreated (Control; left panels), treated with NuBCP-9 R8 (middle panels) or NuBCP-9 PLA^{72K}-PEG^{4K} NPs (right panels) for the indicated times. B. Quantification of Annexin V and PI staining using cellometer vision of MCF-7 cells treated with the indicated agents for 24 h (open bars) and 48 h (solid bars). The results are expressed as mean±SD of three replicates. C. Total cell lysates from MCF-7 and HepG2 cells were analyzed by immunoblotting with anti-BCL-2. D. Lysates from MCF-7 and HepG2 cells treated with 15

μM NuBCP R8 or NuBCP-9 PLA^{72K}-PEG^{4K} NPs for the indicated times were analyzed by immunoblotting with anti-caspase-3 and anti-β-actin. CF: cleaved fragment.

NIH-PA Author Manuscript
NIH-PA Author Manuscript
NIH-PA Author Manuscript

NIH-PA Author Manuscript
NIH-PA Author Manuscript
NIH-PA Author Manuscript

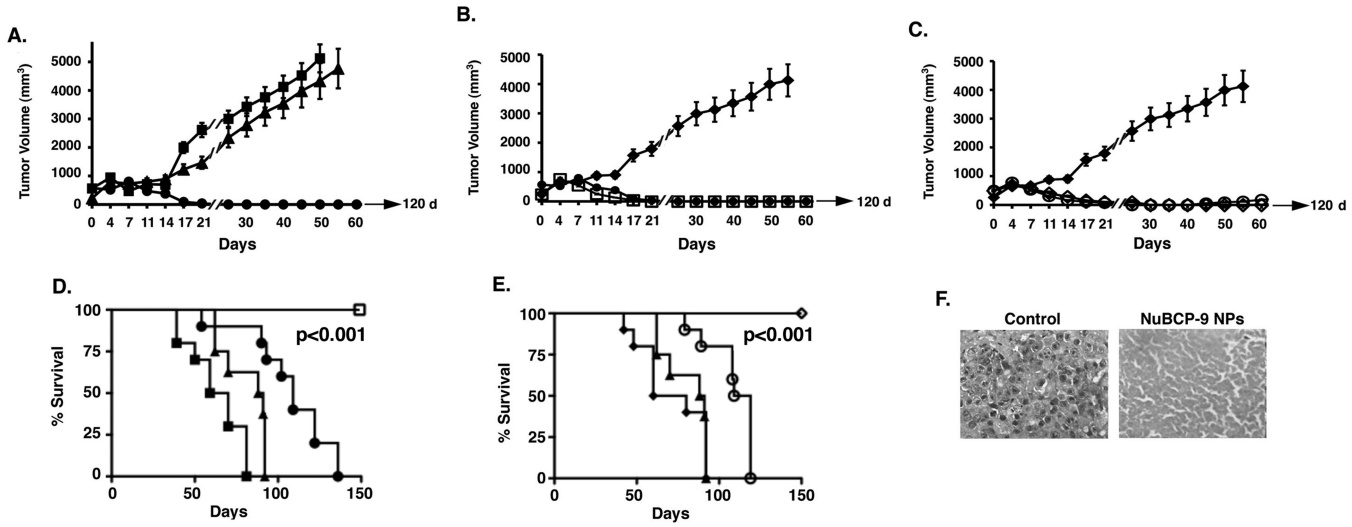

Figure 5. Anti-tumor activity of NuBCP-9 NPs

A. Ehrlich tumor bearing mice were treated with: PBS (IP, closed squares, twice weekly); 20 mg/kg NuBCP-9 (IP, closed triangles, twice weekly) or 20 mg/kg NuBCP-9 PLA^{72K}-PEG^{4K} NPs (IP, closed circles, twice weekly) for a 21 day cycle. Tumor measurements were performed on the indicated days. The results are expressed as tumor volumes (mean±SD). B. Ehrlich tumor bearing mice were treated with: empty PLA^{72K}-PEG^{4K} NPs (IP, closed diamonds, twice weekly); 20 mg/kg NuBCP-9 PLA^{72K}-PEG^{4K} NPs (IP, open squares, once weekly) or 20 mg/kg NuBCP-9 PLA^{72K}-PEG^{4K} NPs (IP, closed circles, twice weekly) for a 21 day cycle. Tumor measurements were performed on the indicated days. The results are expressed as tumor volumes (mean+SD). C. Ehrlich tumor bearing mice were treated with: empty PLA^{72K}-PEG^{4K} NPs (IP, closed diamonds, twice weekly); 20 mg/kg NuBCP-9 PLA^{72K}-PEG-PPG-PEG NPs (IP, open diamonds, twice weekly) or 20 mg/kg NuBCP-9 PLA^{72K}-PEG-PPG-PEG NPs (IT, open circles, twice weekly) for 21 day cycle. Tumor measurements were performed on the indicated days. The results are expressed as tumor volumes (mean±SD). D. The results are expressed as the percentage survival as determined by Kaplan-Meier analysis PBS (closed squares); NuBCP-9 (closed triangles); NuBCP-9 PLA^{72K}-PEG^{4K} NPs (closed circles; IT, weekly) and NuBCP-9 PLA^{72K}-PEG^{4K} NPs (open squares; IP, weekly). The statistical analysis was performed between the vehicle control and the NuBCP-9 PLA-PEG NP group ($p<0.001$). E. The results are expressed as the percentage survival as determined by Kaplan-Meier analysis empty PLA^{72K}-PEG^{4K} NPs (closed diamonds); NuBCP-9 (closed triangles); PLA^{72K}-PEG-PPG-PEG NPs (open circles; IT, twice weekly) and PLA^{72K}-PEG-PPG-PEG NPs (open diamonds; IP, twice weekly). The statistical analysis was performed between the empty PLA-PEG NP group and the NuBCP-9 PLA-PEG-PPG-PEG NP group ($p<0.001$). F. Histopathology of tumor tissues obtained from mice treated with the control (left) or NuBCP-9 PLA^{72K}-PEG^{4K} NPs (right) for 14 days and stained with H&E (× 400).

NIH-PA Author Manuscript
NIH-PA Author Manuscript
NIH-PA Author Manuscript

Table 1

Characterization and physicochemical properties of PLA-PEG block copolymers and nanoparticles

Sample	GPC of copolymers[a]			Hydrodynamic diameter[b], nm	Zeta Potential (ζ)	Peptide/polymer ratio[c] (w/w)	EE[d]%	Particle Size after peptide loading[b], nm	Zeta Potential after peptide loading (ζ)
	Mn	Mw	Mw/Mn						
PLA	59745	72487	1.213	125±3.7	−15.8±1.45	1:10	42.93	132±2.3	−30.07±2.56
PLA-PEG^{1K}	67916	72806	1.072	120±2.5	−10.2±2.04	1:10	52.09	115±3.2	−25.26±4.01
PLA-PEG^{2K}	70692	73485	1.040	117±3.9	−4.7±1.09	1:10	58.96	119±2.7	−20.74±3.10
PLA-PEG^{4K}	72479	78416	1.082	114±1.9	−3.3±0.95	1:10	65.55	111±4.6	−22.90±1.54
PLA-PEG-PPG-PEG$^{12\text{-}5K}$	80256	85678	1.066	120±2.3	−3.1±1.23	1:10	64.04	118±2.5	−21.14±2.45
PLA^{12K}-PEG-PPG-PEG^{125K}	11234	12676	1.182	106±2.7	N.D.	1.:10	56.12	N.D.	N.D.

N.D. Not done

[a] Gel permeation chromatography (GPC) of PLA-PEG block copolymers at room temperature using Viscoteck GPC system with THF as mobile phase

[b] Measured by NTA (Nanoparticle Tracking Analysis; NS500, Nanosight)

[c] Concentration of the polymer was taken as 20 mg/ml

[d] Encapsulation efficiency expressed as a percentage mean of 3 determinants ± S.D. of NuBCP-9 recovered in NPs compared with theoretical load

NIH-PA Author Manuscript

NIH-PA Author Manuscript

NIH-PA Author Manuscript

Table 2

IC_{50} of NuBCP-9 encapsulated PLA-PEG NP's

	MCF-7	HepG2
	IC_{50} (μM)	
NuBCP-9-PLA	2.58	4.18
NuBCP-9-PLA-PEG^{1K}	2.31	3.90
NuBCP-9-PLA-PEG^{2K}	1.90	2.39
NuBCP-9-PLA-PEG^{4K}	2.15	2.03
NuBCP-9-PLA-PEG-PPG-PEG^{125K}	2.00	*ND
NuBCP-9-R8	7.11	9.10

*ND-Not done